

# Static sensitivity of whole-room indirect calorimeters

Gabriele Bandini  
Department of Energy, Systems,  
Territory and Constructions  
Engineering, University of Pisa  
Pisa, Italy  
[gabriele.bandini@ing.unipi.it](mailto:gabriele.bandini@ing.unipi.it)

Alberto Landi  
Department of Information  
Engineering, University of Pisa  
Pisa, Italy  
[alberto.landi@unipi.it](mailto:alberto.landi@unipi.it)

Ferruccio Santini  
Department of Clinical and  
Experimental Medicine,  
University Hospital of Pisa  
Pisa, Italy  
[ferruccio.santini@unipi.it](mailto:ferruccio.santini@unipi.it)

Alessio Basolo  
Department of Clinical and  
Experimental Medicine,  
University Hospital of Pisa  
Pisa, Italy  
[alessio.basolo@med.unipi.it](mailto:alessio.basolo@med.unipi.it)

Mirko Marracci  
Department of Energy, Systems,  
Territory and Constructions  
Engineering, University of Pisa  
Pisa, Italy  
[mirko.marracci@unipi.it](mailto:mirko.marracci@unipi.it)

Paolo Piaggi  
Department of Information  
Engineering, University of Pisa  
Pisa, Italy  
[paolo.piaggi@unipi.it](mailto:paolo.piaggi@unipi.it)

**Abstract**— Whole-room indirect calorimeters (WRIC) are accurate tools to precisely measure energy metabolism in humans via calculation of oxygen consumption and carbon dioxide production. Yet, overall accuracy of metabolic measurements relies on the validity of the theoretical model for gas exchange inside the WRIC volume in addition to experimental and environmental conditions that contribute to the uncertainty of WRIC outcome variables. The aim of this study was to quantitatively study the static sensitivity of a WRIC operated in a push configuration and located at the laboratories of the University Hospital of Pisa with the goal to identify the experimental conditions required to reach the best degree of accuracy for outcome metabolic measurements. Herein we demonstrate that achieving a fractional concentration of carbon dioxide inside the WRIC  $>0.2\%$  at the steady state conditions allows to obtain a relative uncertainty  $<5\%$  for the outcome metabolic measurements.

**Keywords**— Sensitivity analysis, static sensitivity, energy metabolism, indirect calorimetry, metabolic chamber

## I. INTRODUCTION

Whole-room indirect calorimeters (WRIC) are increasingly used devices to precisely measure the rate of energy expenditure in humans via calculation of oxygen ( $O_2$ ) consumption and carbon dioxide ( $CO_2$ ) production [1, 2]. The accurate assessment of human energy metabolism by WRIC systems allows the characterization of each person's metabolic phenotype informative for the individual susceptibility to weight gain and obesity [3, 4]. On the basis of an established dynamic WRIC model for gas exchange [5-7] and known WRIC air volume, the rates of oxygen consumed ( $\dot{V}O_2$ ) and carbon dioxide produced ( $\dot{V}CO_2$ ) by an individual inside a WRIC operating in a push (or pull) configuration can be calculated upon measurements of air inflow (or outflow) rate and fractional concentrations of  $O_2$  and  $CO_2$  both in inflow air and in WRIC air. Accordingly, the overall uncertainty of  $\dot{V}O_2$

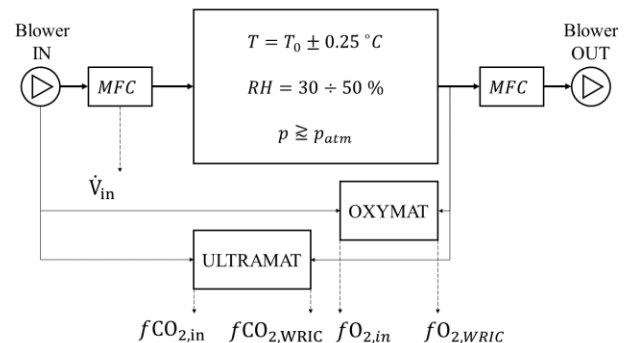


Figure 1. Schematic representation of a whole-room indirect calorimeter (push-pull configuration) showing measured quantities.

and  $\dot{V}CO_2$  estimates relies on the uncertainty of measurements of air flow rate by mass flow meter/controller and  $O_2$  and  $CO_2$  concentrations by gas analyzers, which ultimately impact also the uncertainty of metabolic rate calculated by applying indirect calorimetry equations to  $\dot{V}O_2$  and  $\dot{V}CO_2$  measurements. For instance, unpredictable variations in  $O_2$  and  $CO_2$  concentrations in fresh air due to environmental influences [8] or in WRIC air during the course of experiments may propagate through the WRIC model equations and constitute a source of error for  $\dot{V}O_2$  and  $\dot{V}CO_2$  estimates. Quantifying the impact of each WRIC variable on outcome measurements may provide insight into the best experimental conditions that can minimize the effects of measurements errors and model uncertainties to ensure more accurate estimates of outcome metabolic quantities [9]. In fact, air inflow rate can be precisely adjusted by a mass flow controller (or by a voltage-controlled blower) in a push-calorimeter to ultimately achieve a steady-state value for the

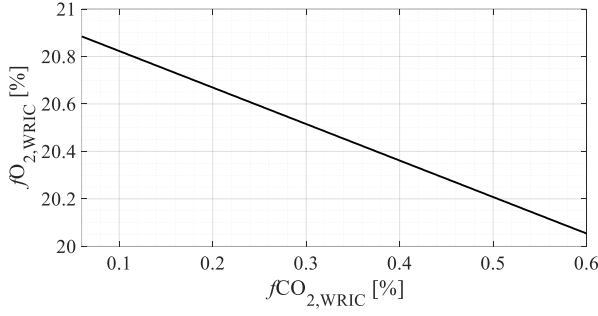


Figure 2. Relationship between  $\text{CO}_2$  concentration versus  $\text{O}_2$  concentration inside the WRIC at the steady-state for  $RQ = 0.6$ .

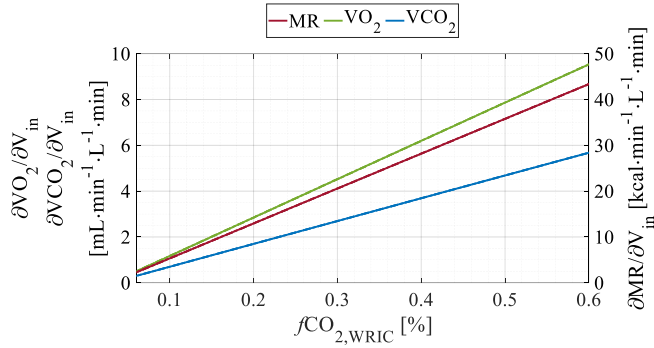


Figure 3. Partial derivatives of MR (right y-axis),  $\dot{V}\text{O}_2$  and  $\dot{V}\text{CO}_2$  (left y axis) with respect to air inflow rate versus  $f\text{CO}_{2,\text{WRIC}}$  (x axis).

fractional concentration of  $\text{CO}_2$  inside the WRIC [7, 10]. Yet, the quantification of uncertainty in outcome WRIC measurements arising from the uncertainty in inflow rate and  $\text{CO}_2$  measurements is warranted to identify the optimal experimental conditions for these two WRIC variables. The aim of the present study was to conduct a formal sensitivity analysis of WRIC model for gas exchange in steady-state conditions to quantify the impact of each WRIC system variable on the uncertainty of  $\dot{V}\text{O}_2$  and  $\dot{V}\text{CO}_2$  outcome measurements.

## II. METHODS

### A. Static sensitivity of steady-state WRIC dynamic model

A schematic representation of a WRIC operated in a push-pull configuration is shown on Figure 1. including the most important components, parameters, and measured quantities. The steady-state (static) equations for  $\dot{V}\text{O}_2$  and  $\dot{V}\text{CO}_2$  measurements [mL/min] of an individual residing inside the WRIC are the following:

$$\begin{aligned} \dot{V}\text{O}_2 &= -\dot{V}_{in} \times (f\text{O}_{2,\text{WRIC}} \times H - f\text{O}_{2,in}) \times 10 \\ \dot{V}\text{CO}_2 &= \dot{V}_{in} \times (f\text{CO}_{2,\text{WRIC}} \times H - f\text{CO}_{2,in}) \times 10 \end{aligned} \quad (1)$$

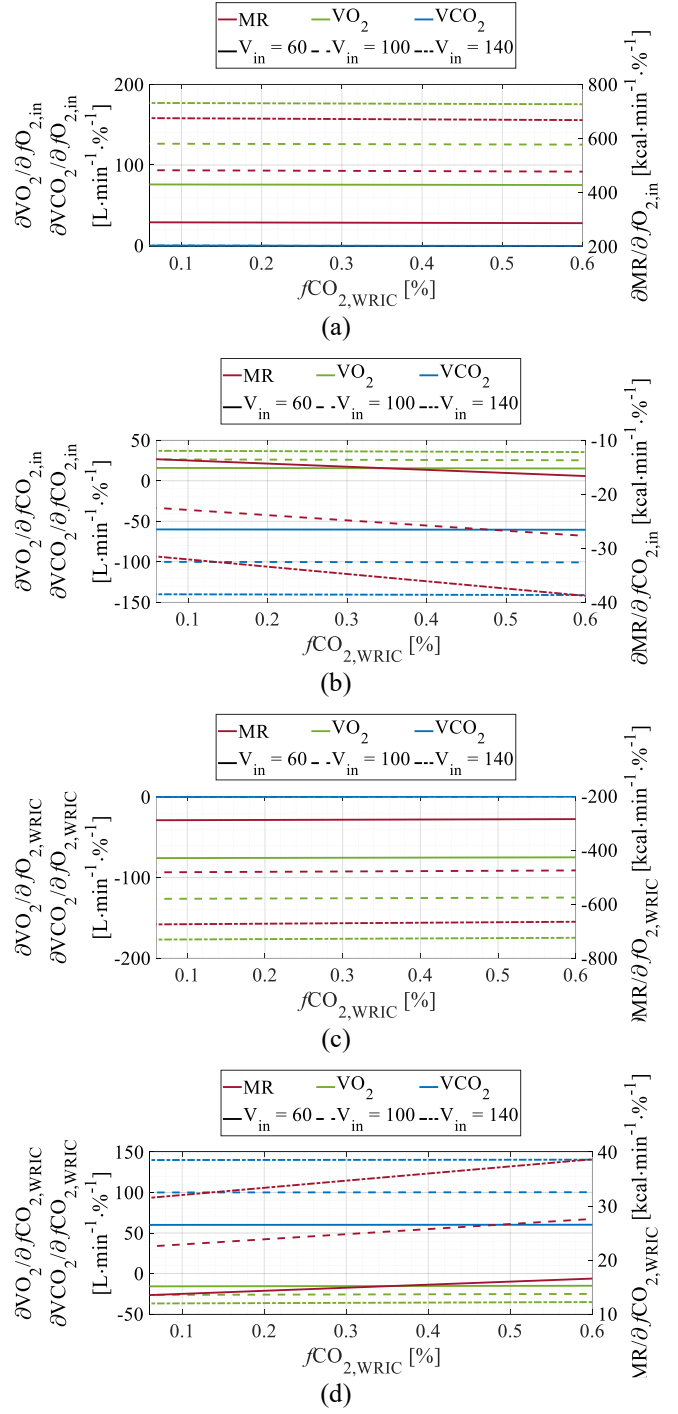


Figure 4. Partial derivatives of MR (right y-axis),  $\dot{V}\text{O}_2$  and  $\dot{V}\text{CO}_2$  (left y axis) with respect to  $f\text{O}_{2,in}$  (a),  $f\text{CO}_{2,in}$  (b),  $f\text{O}_{2,\text{WRIC}}$  (c), and  $f\text{CO}_{2,\text{WRIC}}$  (d) versus  $f\text{CO}_{2,\text{WRIC}}$  (x axis) for three different values of  $\dot{V}_{in}$ .

where  $\dot{V}_{in}$  is the air inflow rate [L/min] while  $f\text{O}_{2,in}$  and  $f\text{CO}_{2,in}$  and  $f\text{O}_{2,\text{WRIC}}$  and  $f\text{CO}_{2,\text{WRIC}}$  are the fractional concentrations of  $\text{O}_2$  and  $\text{CO}_2$  (expressed as percentage) in inflow air and inside the WRIC, respectively



Figure 5. Instrumentation rack hosting the gas analyzers.

[7]. The quantity  $H$  is the Haldane factor based on nitrogen balance in fresh and WRIC air:

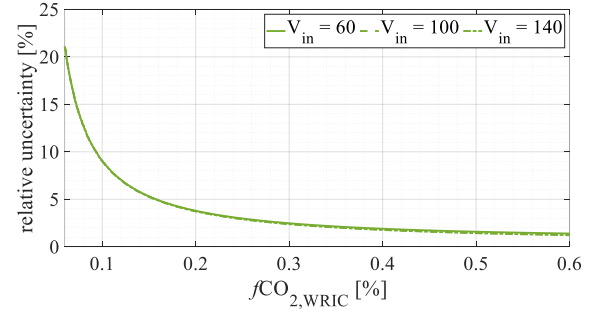
$$H = \frac{100\% - fO_{2,in} - fCO_{2,in}}{100\% - fO_{2,WRIC} - fCO_{2,WRIC}} \quad (2)$$

In our data simulations, the fractional concentrations of  $O_2$  and  $CO_2$  in inflow air ( $fO_{2,in}$  and  $fCO_{2,in}$ ) were assumed to be constant at 20.93% and 0.03%, respectively. The respiratory quotient (RQ), calculated as the ratio of  $\dot{V}CO_2$  divided by  $\dot{V}O_2$ , was set to 0.6 to simulate the expected RQ of a chemically pure propane burn, commonly used for WRIC validation tests [9]. The metabolic rate (MR, kcal/min) was derived using the Lusk's equation on the basis of  $\dot{V}O_2$  and RQ:

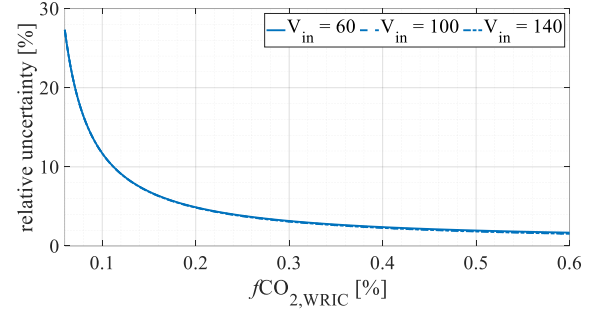
$$RQ = \frac{\dot{V}CO_2}{\dot{V}O_2}$$

$$MR = \dot{V}O_2 \times [4.686 + (RQ - 0.707) \times 1.2321] \quad (3)$$

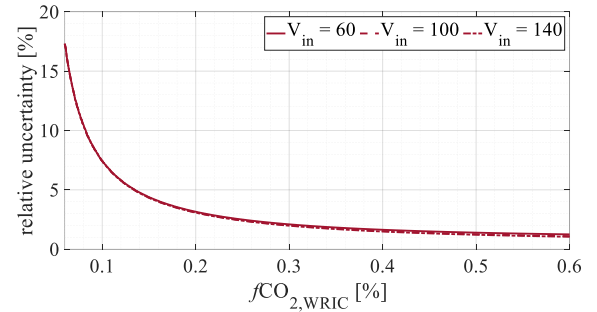
Assuming constrained values for  $O_2$  and  $CO_2$  concentrations in inflow air as well as for RQ, the WRIC steady-state model can be studied by varying the values for air inflow rate  $\dot{V}_{in}$  and  $CO_2$  concentration inside the WRIC to evaluate their impact on outcome  $\dot{V}O_2$ , and  $\dot{V}CO_2$  estimates. Being the RQ independent from  $\dot{V}_{in}$ , setting a value for RQ consequently constrains the value of  $fCO_{2,WRIC}$  once a value for  $fCO_{2,WRIC}$  has been chosen (Figure 2). The whole WRIC model is thus described as a function both of  $\dot{V}_{in}$  and  $fCO_{2,WRIC}$ .



(a)  $\dot{V}O_2$



(b)  $\dot{V}CO_2$



(c) MR

Figure 6. Trends of relative uncertainty for  $\dot{V}O_2$  (a),  $\dot{V}CO_2$  (b), and MR (c) as a function of  $fCO_{2,WRIC}$  (x axis) for three different values of  $\dot{V}_{in}$ .

For a full characterization of outcome WRIC measurements at the steady state, the measurement uncertainty in inflow rate and gas concentrations must be taken into account and propagated through the equations (1), (2) and (3). The sensitivity analysis of WRIC model is important in order to possibly minimize uncertainty for  $\dot{V}O_2$  and  $\dot{V}CO_2$  enhancing the accuracy of outcome metabolic measurements (RQ and MR). Based on the Haldane factor and Lusk's equation, the partial derivatives can be analytically derived with respect to the measured quantities. We assume the input quantities of WRIC model (inflow rate and gas concentrations) to be uncorrelated in the normal operation of the WRIC. Then, it is possible to propagate the measurement uncertainty of the measured quantities with a first-order Taylor series approximation of the WRIC model, as recommended by the GUM [11].

The values of partial derivatives that linearize the WRIC model around the operating point at the steady-state conditions

Table 1. Steady-state values, absolute and relative uncertainty for the studied quantities.

L/min	%	ratio	%	%	%	Steady-state values			Absolute uncertainty			Relative uncertainty [%]		
$\dot{V}_{in}$	$f_{CO_2,WRIC}$	RQ	$f_{O_2,in}$	$f_{CO_2,in}$	$f_{O_2,WRIC}$	$\dot{V}O_2$ [L/min]	$\dot{V}CO_2$ [L/min]	MR [kcal/min]	$\dot{V}O_2$ [mL/min]	$\dot{V}CO_2$ [mL/min]	MR [kcal/min]	$\dot{V}O_2$	$\dot{V}CO_2$	MR
60	0.064	0.6	20.93	0.03	20.88	0.034	0.020	0.155	6.3	4.9	23.7	18.6	24.1	15.3
100	0.064	0.6	20.93	0.03	20.88	0.057	0.034	0.258	10.5	8.2	39.4	18.6	24.1	15.3
140	0.064	0.6	20.93	0.03	20.88	0.079	0.048	0.362	14.8	11.4	55.2	18.6	24.0	15.3
60	0.2	0.6	20.93	0.03	20.67	0.171	0.102	0.777	6.5	5.0	24.5	3.8	4.9	3.2
100	0.2	0.6	20.93	0.03	20.67	0.285	0.170	1.296	10.7	8.3	40.1	3.7	4.9	3.1
140	0.2	0.6	20.93	0.03	20.67	0.399	0.238	1.814	14.9	11.5	55.9	3.7	4.8	3.1
60	0.5	0.6	20.93	0.03	20.21	0.472	0.281	2.146	7.5	5.5	29.9	1.6	2.0	1.4
100	0.5	0.6	20.93	0.03	20.21	0.786	0.468	3.577	11.6	8.7	45.2	1.5	1.9	1.3
140	0.5	0.6	20.93	0.03	20.21	1.101	0.656	5.007	15.8	12.0	60.9	1.4	1.8	1.2

are shown in Figure 3 and Figure 4, where the values referring to  $\dot{V}O_2$  and  $\dot{V}CO_2$  are reported on the left axis while those referring to MR are reported on the right axis. The absolute rates of change of these outcome measurements do not largely depend on the air inflow rate value  $\dot{V}_{in}$ , whereas they increase as the fractional concentration of  $CO_2$  inside the WRIC increases. Assuming  $\dot{V}CO_2$  and  $\dot{V}O_2$  to be positive values as calculated in (1), the partial derivatives with respect to the fractional concentrations of  $CO_2$  inside the WRIC are shown on Figure 4. The derivatives referring to the same  $O_2$  or  $CO_2$  concentrations in fresh air (panels a-b) and in WRIC air (panels c-d) have opposite signs and are mirrored with respect to the x-axis. In all cases, the derivatives values grow linearly with  $\dot{V}_{in}$ .

While the uncertainty value on the measurand is related to the uncertainty contributions from the measurements on the model input quantities, those partial derivatives represent the parameters of propagation of those uncertainties and are only related to the specific WRIC model used. In the following, the metabolic chamber at the University Hospital of Pisa is taken as example to study the propagation of uncertainty with real-case values for input quantities based on specific instrumentations.

### III. RESULTS

#### A. Uncertainty analysis

The metabolic chamber at the University Hospital of Pisa, Italy [12] is 3.60 m long, 3.00 m wide, and 2.70 m high (total volume of 29.16 m<sup>3</sup>). The chamber has climate control, with an air conditioning (HVAC) system utilizing chilled water pipelines and electric heating coils to maintain temperature within 0.5°C and relative humidity within 30% ÷ 50% (Figure 1). Sample of WRIC air is drawn by membrane pumps, dried to a humidity level <1,000 ppm using a gas sample dryer (Perma Pure LLC) driven by counterflowing dry medical air, and then sent to absolute gas analyzers (Siemens Ultramat/ Oxymat 6). A voltage-controlled blower (Ametek, Windjammer) draws fresh air from outside the building and the inflow rate to the WRIC is finely tuned by a mass flow controller (Teledyne Hastings Instruments, Digital 300 series, range: 300 L/min).

The overall declared accuracy of mass flow controller can be expressed as:

$$\pm(0.2\% \text{ full scale} + 0.5\% \text{ of reading}) \quad (4)$$

Figure 5 shows the instrumentation rack hosting the two gas analyzers (Siemens Ultramat/Oxymat 6) used to measure the  $O_2$  and  $CO_2$  concentrations both in fresh air and WRIC air. The Ultramat gas analyzer operates according to the infrared two-beam alternating light principle, measuring the gases whose absorption bands lie within the infrared wavelength range from 2  $\mu\text{m}$  to 9  $\mu\text{m}$ . In our laboratory, this analyzer cell is used to measure  $CO_2$  concentration. Concerning the  $O_2$  concentration, this is measured with the Oxymat cell, whose principle of operation is based on the paramagnetic alternating pressure principle. Before each WRIC experiment, both cells of gas analyzers are calibrated with two-point linear equation using tanks containing gases with known concentrations. Specifically, the Oxymat cell is calibrated between 20% and 21% while the Ultramat cell is calibrated in the  $CO_2$  range 0 ÷ 10,000 ppm (0% ÷ 1%). The maximum declared error both for  $O_2$  and  $CO_2$  concentrations is reported by the manufacturer to be:

$$\pm(1\% \text{ of measuring range}) \quad (5)$$

where the measuring range for  $O_2$  and  $CO_2$  concentrations was 1% for both cells. Consequently, assuming a uniform distribution for errors, the resulting uncertainty for  $O_2$  and  $CO_2$  concentrations can be evaluated as 1% divided by  $\sqrt{3}$ .

The propagation of uncertainty values reported in (4) and (5) through the equations of WRIC model described by (1), (2) and (3) leads to the relative uncertainty values shown in Figure 6. In our simulations, the values for  $\dot{V}_{in}$  ranged from 60 to 140 L/min, while  $CO_2$  concentration inside the WRIC,  $f_{CO_2,WRIC}$ , ranged from 0.06% to 0.6%. Accordingly,  $f_{O_2,WRIC}$  was constrained to the corresponding value shown on Figure 2 after setting a RQ = 0.6. Considering the general quantity K with its

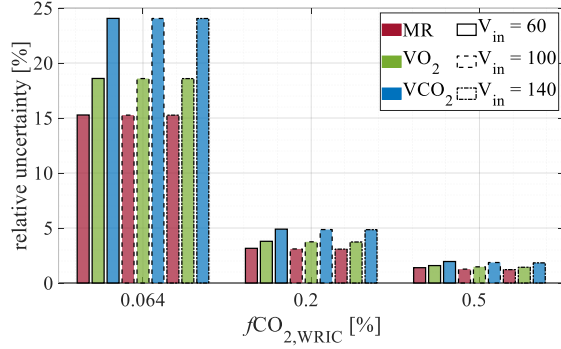
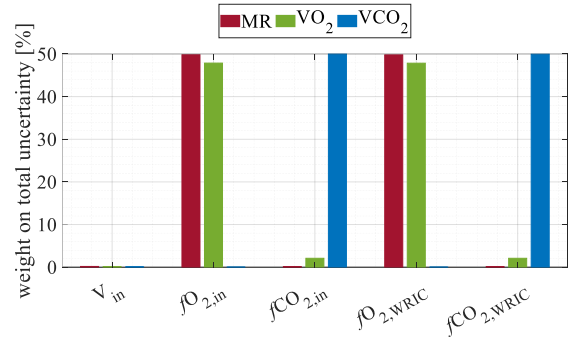


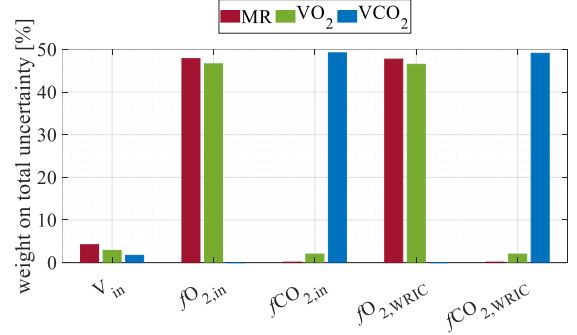
Figure 7. Relative uncertainty of  $\dot{V}O_2$ ,  $\dot{V}CO_2$ , and MR estimates for different values of air inflow rate (60, 100, 140 L/min) and  $CO_2$  concentration (0.064, 0.2, 0.5%) inside the WRIC.

uncertainty  $u(K)$ , the relative uncertainty is derived as  $u(K)/K$  for each operating point of the model, i.e., for each combination of  $V_{in}$  and  $fCO_{2,WRIC}$ , given the value of other quantities in the model. For each of the three outcome quantities ( $\dot{V}O_2$ ,  $\dot{V}CO_2$ , and MR), the trend of the relative uncertainty as a function both of  $V_{in}$  and  $fCO_{2,WRIC}$  was similar (Figure 6). The relative uncertainty of all three outcome estimates was practically unaffected by differences in air inflow rate  $V_{in}$  as can be noted by the superimposition of the three curves for 60-100-140 L/min in each panel. Conversely, there was a substantial, nonlinear influence of  $fCO_{2,WRIC}$  on the relative uncertainty of each of the three outcome estimates, such that a relatively higher values for outcome uncertainty ( $>5\%$ ) was observed at relatively lower values ( $<0.1\%$ ) of  $fCO_{2,WRIC}$ . Because during WRIC experiments (e.g., propane burn)  $fCO_{2,WRIC}$  typically increases from fresh air levels ( $\sim 0.03\%$ ) to values  $>0.2\%$  as a result of an ongoing combustion inside the WRIC, the corresponding relative uncertainty of outcome measurements may decrease over time from 15-30% to values well below 5%, respectively. Taken together, these results indicate that the main WRIC system variable to be controlled in order to minimize the effect of measurement uncertainty on outcome quantities is the fractional concentration of  $CO_2$  inside the WRIC.

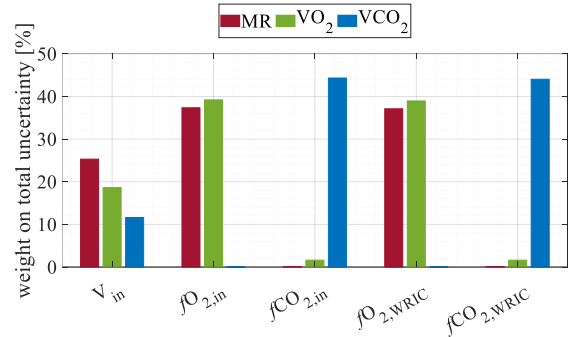
To quantify and summarize this main result, Table 1 shows both absolute and relative uncertainty values for specific values of  $V_{in}$  and  $fCO_{2,WRIC}$ . In particular, three arbitrary values (low, intermediate, high) were chosen across the experimental range both for  $V_{in}$  (60 L $\cdot$ min $^{-1}$ , 100 L $\cdot$ min $^{-1}$ , and 140 L $\cdot$ min $^{-1}$ ) and  $fCO_{2,WRIC}$  (0.064%, 0.2% and 0.5%). These results are summarized in Figure 7. Overall, the relative uncertainty of  $\dot{V}CO_2$  was higher than that of  $\dot{V}O_2$  or MR. As also observed above, differences in inflow rate  $V_{in}$  had an almost negligible impact on relative uncertainty of all three outcome measurements. Conversely, there was a strong effect of  $CO_2$  concentration inside the WRIC on all uncertainties, such that all relative uncertainty values substantially decreased below 5% at a value of 0.2% for  $fCO_{2,WRIC}$  and further below 2% ( $\sim 1\%$  for MR) at a value of 0.5% for  $fCO_{2,WRIC}$ .



(a)  $fCO_{2,WRIC} = 0.064\%$



(b)  $fCO_{2,WRIC} = 0.2\%$



(c)  $fCO_{2,WRIC} = 0.5\%$

Figure 8. Weight (%) of each WRIC measured variable to total uncertainty of  $\dot{V}O_2$ ,  $\dot{V}CO_2$ , and MR estimates for three different values of  $fCO_{2,WRIC}$ .

### B. Weight of uncertainty sources

Assuming a value of 100 L $\cdot$ min $^{-1}$  for air inflow rate, the weight of each contribution to uncertainty on  $\dot{V}O_2$ ,  $\dot{V}CO_2$ , and MR can be quantified. For instance, the uncertainty of MR can be written based on a linear approximation of the WRIC model assuming no correlation between quantities as:

$$u(MR)^2 = C(V_{in})^2 + C(fO_{2,in})^2 + C(fCO_{2,in})^2 + C(fO_{2,WRIC})^2 + C(fCO_{2,WRIC})^2 \quad (6)$$

where  $C$  is the contribution which, taking the air inflow rate as an example, can be derived as

$$C(V_{in})^2 = \left( \frac{\partial MR}{\partial V_{in}} \right)^2 \cdot u(V_{in})^2 \quad (7)$$

The ratio between each squared contribution and the squared uncertainty is represented for the three considered values of  $fCO_{2,WRIC}$  in Figure 8, where the bars show the contribution of input quantities (i.e., inflow rate and  $O_2$  and  $CO_2$  measurements both in fresh air and in WRIC air) on outcome uncertainties of  $\dot{V}O_2$ ,  $\dot{V}CO_2$  and MR at three different levels for  $fCO_{2,WRIC}$ . At a low level of 0.064% for  $fCO_{2,WRIC}$  (panel a),  $V_{in}$  has a negligible influence on the overall uncertainty values for all three outcome measurements. For higher values of  $CO_2$  concentration inside the WRIC (panels b and c), the influence of  $V_{in}$  on outcome measurements increases, reaching the value of ~25% for MR uncertainty when  $fCO_{2,WRIC} = 0.5\%$  (panel c).

In addition to the increasing contribution of  $V_{in}$  on MR uncertainty with increasing  $fCO_{2,WRIC}$ , the other contributions to MR uncertainty are ascribable to the fractional concentrations of  $O_2$  (both in inflow air and in WRIC air equally), but not to the fractional concentrations of  $CO_2$  whose impact was negligible at all  $fCO_{2,WRIC}$  values. In summary, not only it is recommended to promptly reach a steady-state value for higher  $fCO_{2,WRIC}$  (e.g., 0.5% at the midpoint of calibration curve) to minimize the relative uncertainty on the outcome measurements as shown in Figure 8, but also to accurately measure air inflow rate  $V_{in}$  and  $O_2$  concentrations as they collectively constitute the main contributions to the final uncertainty of MR measurements.

#### IV. CONCLUSIONS

In this paper, we analytically studied the static sensitivity of whole-room indirect calorimeters operating in a push configuration to quantify the contributions of air flow rate and measurements of gas concentration on outcome WRIC measurements ( $\dot{V}O_2$ ,  $\dot{V}CO_2$  and MR). We demonstrated that achieving a  $CO_2$  concentration inside the calorimeter greater than 0.2% at the steady state condition allows to obtain a relative uncertainty smaller than 5% for the outcome metabolic measurements.

#### ACKNOWLEDGMENTS

This research was supported by PRIN 2017L8Z2EM\_002 ("Mechanisms of adipose tissue

dysfunction in obesity: a target of future weight loss strategies for the prevention of diabetes and cardiovascular diseases") from the Italian Minister of Education and Research and by RF-2010-2310538 ("Building a state of the art whole room indirect calorimeter, a tool to accurately investigate the role of energy expenditure and substrate oxidation in endocrine and metabolic disorders") from the Italian Minister of Health. Dr. Paolo Piaggi was supported by the program "Rita Levi Montalcini for young researchers" from the Italian Minister of Education and Research.

#### REFERENCES

- [1] Y. Y. Lam and E. Ravussin, "Indirect calorimetry: an indispensable tool to understand and predict obesity," *Eur J Clin Nutr*, vol. 71, pp. 318-322, Mar 2017.
- [2] Y. Y. Lam and E. Ravussin, "Analysis of energy metabolism in humans: A review of methodologies," *Mol Metab*, vol. 5, pp. 1057-1071, Nov 2016.
- [3] P. Piaggi, "Metabolic Determinants of Weight Gain in Humans," *Obesity (Silver Spring)*, vol. 27, pp. 691-699, May 2019.
- [4] P. Piaggi, K. L. Vinales, A. Basolo, F. Santini, and J. Krakoff, "Energy expenditure in the etiology of human obesity: spendthrift and thrifty metabolic phenotypes and energy-sensing mechanisms," *J Endocrinol Invest*, vol. 41, pp. 83-89, Jan 2018.
- [5] D. Brown, T. J. Cole, M. J. Dauncey, R. W. Marrs, and P. R. Murgatroyd, "Analysis of gaseous exchange in open-circuit indirect calorimetry," *Med Biol Eng Comput*, vol. 22, pp. 333-8, Jul 1984.
- [6] M. Sun, G. W. Reed, and J. O. Hill, "Modification of a whole room indirect calorimeter for measurement of rapid changes in energy expenditure," *J Appl Physiol (1985)*, vol. 76, pp. 2686-91, Jun 1994.
- [7] J. K. Moon, F. A. Vohra, O. S. Valerio Jimenez, M. R. Puyau, and N. F. Butte, "Closed-loop control of carbon dioxide concentration and pressure improves response of room respiration calorimeters," *J Nutr*, vol. 125, pp. 220-8, Feb 1995.
- [8] E. L. Melanson, J. P. Ingebrigtsen, A. Bergouignan, K. Ohkawara, W. M. Kohrt, and J. R. Lighton, "A new approach for flow-through respirometry measurements in humans," *Am J Physiol Regul Integr Comp Physiol*, vol. 298, pp. R1571-9, Jun 2010.
- [9] K. Y. Chen, S. Smith, E. Ravussin, J. Krakoff, G. Plasqui, S. Tanaka, et al., "Room Indirect Calorimetry Operating and Reporting Standards (RICORS 1.0): A Guide to Conducting and Reporting Human Whole-Room Calorimeter Studies," *Obesity (Silver Spring)*, vol. 28, pp. 1613-1625, Sep 2020.
- [10] E. Ravussin, S. Lillioja, T. E. Anderson, L. Christin, and C. Bogardus, "Determinants of 24-hour energy expenditure in man. Methods and results using a respiratory chamber," *J Clin Invest*, vol. 78, pp. 1568-78, Dec 1986.
- [11] J. Jcgm, "Evaluation of measurement data—Guide to the expression of uncertainty in measurement," *Int. Organ. Stand. Geneva ISBN*, vol. 50, p. 134, 2008.
- [12] P. Piaggi, A. Landi, F. Santini, and M. Marracci, "Construction and set-up of a whole-room indirect calorimeter for measurement of human energy metabolism," pp. 1-5, 2020.